Regional knockdown of NDUFS4 implicates a thalamocortical circuit mediating anesthetic sensitivity

Renjini Ramadasan-Nair[1]*, Jessica Hui[1], Pavel I. Zimin[1,2], Leslie S. Itsara[1], Philip G. Morgan[1,2], Margaret M. Sedensky[1,2]

1 Center for Integrative Brain Research, Seattle Children's Research Institute, 1900 Ninth Avenue, Seattle, WA, United States of America, **2** Department of Anesthesiology and Pain Medicine, University of Washington, Seattle, WA, United States of America

* renjini.ramadasannair@seattlechildrens.org

Abstract

Knockout of the mitochondrial complex I protein, NDUFS4, profoundly increases sensitivity of mice to volatile anesthetics. In mice carrying an $Ndufs4^{lox/lox}$ gene, adeno-associated virus expressing Cre recombinase was injected into regions of the brain postulated to affect sensitivity to volatile anesthetics. These injections generated otherwise phenotypically wild type mice with region-specific, postnatal inactivation of $Ndufs4$, minimizing developmental effects of gene loss. Sensitivities to the volatile anesthetics isoflurane and halothane were measured using loss of righting reflex (LORR) and movement in response to tail clamp (TC) as endpoints. Knockdown (KD) of $Ndufs4$ in the vestibular nucleus produced resistance to both anesthetics for movement in response to TC. $Ndufs4$ loss in the central and dorsal medial thalami and in the parietal association cortex increased anesthetic sensitivity to both TC and LORR. Knockdown of $Ndufs4$ only in the parietal association cortex produced striking hypersensitivity for both endpoints, and accounted for half the total change seen in the global KO ($Ndufs4(KO)$). Excitatory synaptic transmission in the parietal association cortex in slices from $Ndufs4(KO)$ animals was hypersensitive to isoflurane compared to control slices. We identified a direct neural circuit between the parietal association cortex and the central thalamus, consistent with a model in which isoflurane sensitivity is mediated by a thalamic signal relayed through excitatory synapses to the parietal association cortex. We postulate that the thalamocortical circuit is crucial for maintenance of consciousness and is disrupted by the inhibitory effects of isoflurane/halothane on mitochondria.

Introduction

Anesthesia is a complex phenomenon characterized by amnesia, analgesia, immobility and loss of consciousness. Anesthetic mechanisms are not well understood at several levels of neuronal function. These include the molecular binding targets, the disrupted physiological mechanisms, the brain regions involved, and the altered neuronal circuitry systems. Previous reports have shown that defects in mitochondrial complex I profoundly hypersensitize *C. elegans*, mice and children to volatile anesthetics [1–3]. In addition, complex I function is

uniquely sensitive to volatile anesthetics in concentrations that correlate with the whole animal EC_{50}s of the respective species [1, 4, 5].

Mice featuring a global knock out of the mitochondrial protein NDUFS4 display biochemically proven complex I specific mitochondrial dysfunction [6–8]. This animal, *Ndufs4(KO)*, displays the greatest volatile anesthetic hypersensitivity yet reported for any mammal [3]. The sensitivity is recapitulated by glutamate-cell specific KO of the gene in the central nervous system [9]. It is well documented that anesthetics lower the cerebral metabolic rate in an agent- and region-specific manner [10–14]. However, whether this is a cause or effect of the anesthetized state is controversial [15, 16]. Changes in anesthetic sensitivity seen in *Ndufs4(KO)* mice favor the model that a lowered metabolic rate causes the anesthetic state. However, it remains possible that compensatory developmental changes in the constitutive global *Ndufs4(KO)* may also play a role in determining anesthetic sensitivity.

To determine whether the inhibited metabolic state of specific regions of the CNS causes the anesthetic phenotype, and to eliminate early developmental changes resulting from the global loss of *Ndufs4*, we postnatally knocked down *Ndufs4* in specific CNS regions in mice with normal volatile anesthetic sensitivity. Taking cues from current literature [17–19] and the pathogenesis of the global KO [20], *Ndufs4* was separately knocked down in the vestibular nucleus (VN), the mesopontine tegmental area (MPTA), central and dorsal medial thalami (CMT & DMT), and the parietal association cortex (PAC). The contribution of the regional mitochondrial defects on sensitivity to isoflurane (ISO) or halothane (HAL) were evaluated using loss of righting reflex (LORR) and loss of response to a tail clamp (TC) as endpoints. Since loss of the protein NDUFS4 in the PAC caused the largest change in ISO and HAL sensitivity, we investigated the effect of NDUFS4 loss on the sensitivity of excitatory field potentials to ISO in the PAC.

Results

We previously reported the striking hypersensitivity of *Ndufs4* global KO mice to ISO and HAL for the TC assay (S1 Table) [3]. Here, we measured the change in sensitivity of the global KO for loss of righting reflex (LORR). *Ndufs4(KO)* mice were hypersensitive to ISO (EC_{50}(control) 0.96 ±0.08%, EC_{50}(KO) 0.42±0.08%; p = 3.1X10^{-7}) and HAL (EC_{50}(control) 0.95±0.03%, EC_{50}(KO) 0.41±0.05%; p = 1.4X10^{-10}) (S1 Table). Active (WT-Cre) and inactive (Δ-Cre) viruses, each linked to a GFP construct to establish localization, were then injected into five regions of the CNS of *Ndufs4*$^{lox/lox}$ mice (Fig 1A and 1B). Since the half-life of NDUFS4 is around 17 days [21], we performed behavioral testing and histological analyses three weeks after viral injections. Robust knockdown of *Ndufs4* in the regions injected with WT-Cre virus was confirmed by immunohistochemistry (Fig 1C, S1 Fig) at 4 weeks post virus injections. The loss of NDUFS4 immunostaining in the GFP-expressing virus infected cells in the injected regions was quantified to confirm virus mediated knockdown of NDUFS4 (Fig 1D). We found that cells near the periphery of the WT-Cre injected foci, which did not take up the virus, retained the expression of NDUFS4 (S1B Fig). By immunostaining, we found that cytochrome C expression, indicating the presence of mitochondria, remained unaltered in the WT-Cre and Δ-Cre injected regions (S2 Fig).

Vestibular nucleus (VN)

The VN is one of the regions showing maximal pathology in *Ndufs4(KO)* animals and is implicated in locomotor ability and nociceptive signaling [22, 23]. We injected WT-Cre (Fig 2A, 2B and 2C) and Δ-Cre (S3A Fig) bilaterally into the VN. Loss of *Ndufs4* in the VN decreased sensitivity of the mice and caused resistance to both ISO and HAL for TC (Fig 2E, S4B Fig; Table 1). There was no statistically significant difference in the LORR between VN specific KD and control animals for either anesthetic (Fig 2D, S4A Fig; Table 1).
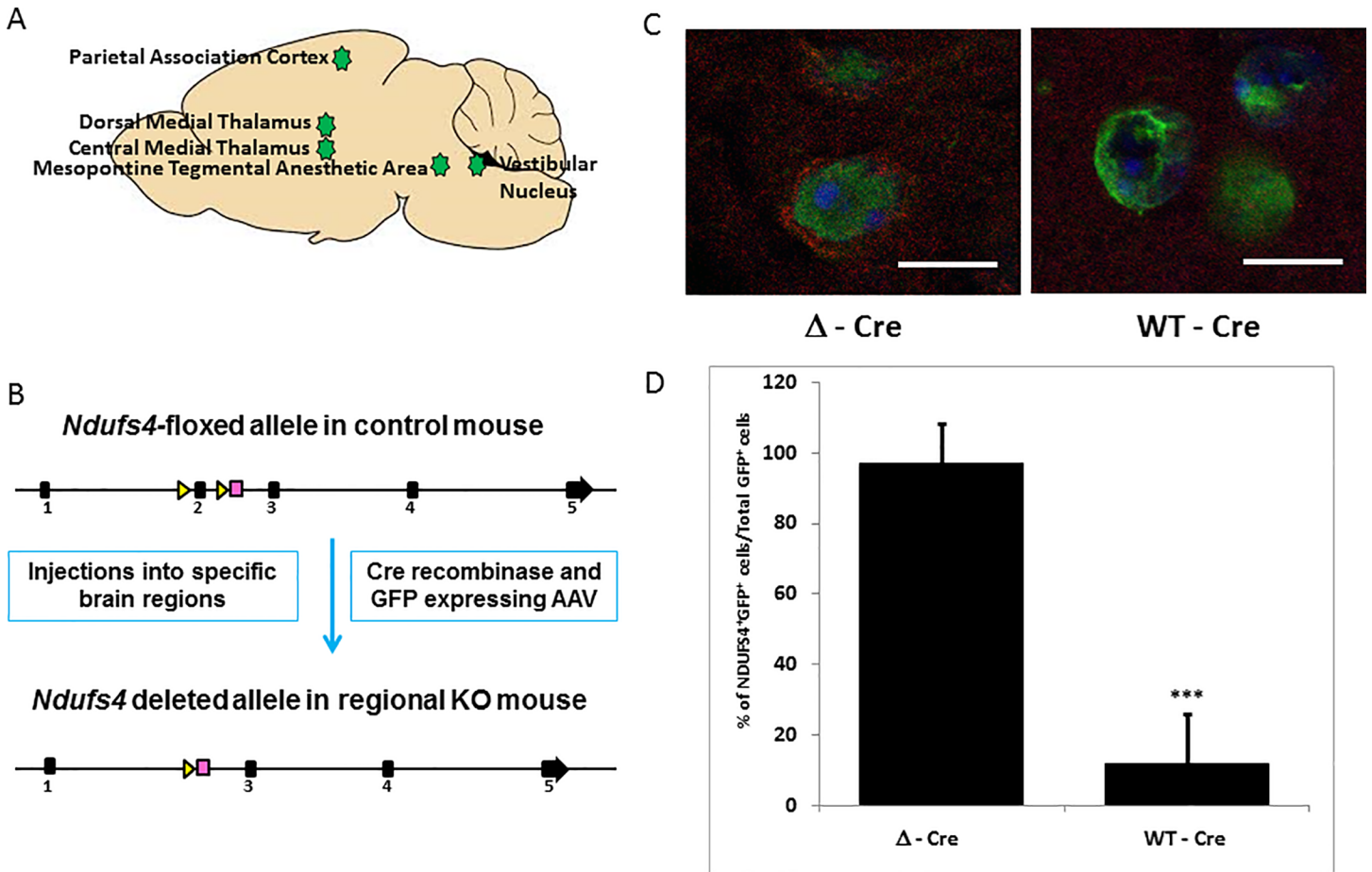
Fig 1. Viral injections and characterization. A. Schematic diagram depicting the five regions which were injected with either rAAV/WT-Cre GFP (knockout virus expressing functional Cre recombinase) or rAAV/Δ-Cre GFP (sham virus expressing nonfunctional Cre recombinase). **B**. Schematic showing the mechanism of gene deletion. Exon 2 of genomic *Ndufs4* is excised by the virus expressing active Cre recombinase, resulting in the loss of NDUFS4 protein as described by Kruse *et al.* [6]. **C**. Loss of *Ndufs4* expression in active Cre virus infected cells in the PAC. Infected cells appear green under the confocal microscope due to the viral GFP co-expression (Magnification X1000). In the Δ-Cre sham virus infected cells of the PAC, mitochondrial NDUFS4 fluorescence (red) is seen, which is absent in the WT-Cre infected cells. **D**. Representative quantitation of NDUFS4 expression in the virus infected cells, shown as a percentage of total infected cells. 20 image fields were quantified per injected locus. Scale bar: 10μm. *** indicates p-values <0.001.

https://doi.org/10.1371/journal.pone.0188087.g001

Mesopontine tegmental area (MPTA)

Based on the data of Devor and colleagues using rats [17], we followed anatomical co-ordinates for mice and injected the WT-Cre (Fig 3A, 3B and 3C) and Δ-Cre viruses (S3B Fig) bilaterally into the calculated mouse brain MPTA. There was no statistically significant change in the TC response of MPTA specific KD to either anesthetic when compared to the sham virus injected group (Fig 3E, S4D Fig; Table 1). While the KDs did not show any change in sensitivity to HAL for LORR, they showed a statistically significant increase in sensitivity to ISO for LORR (Fig 3D, S4C Fig; Table 1).

Central medial thalamus (CMT)

The CMT is critically involved in sensory relaying to the cortex; this region has been shown to play roles in anesthesia [10, 25] and sleep mediation [26]. We injected the WT-Cre (Fig 4A, 4B and 4C) and Δ-Cre (S3C Fig) viruses bilaterally into the CMT. Knocking down *Ndufs4* in the CMT caused hypersensitivity to both ISO and HAL for TC (Fig 4E, S4F Fig; Table 1). Similarly

for LORR, loss of *Ndufs4* in the CMT made mice hypersensitive to ISO and HAL (Fig 4D, S4E Fig; Table 1).

Dorsal medial thalamus (DMT)

The DMT has been implicated in mediolateral pain modulation and anesthesia mediation by pentobarbital [27]. We injected the WT-Cre (Fig 5A, 5B and 5C) and Δ-Cre (S3D Fig) viruses bilaterally into the DMT. Removal of *Ndufs4* caused significant hypersensitivity to both ISO and HALfor TC (Fig 5E, S4H Fig; Table 1). Similarly for LORR, loss of *Ndufs4* in the DMT made mice hypersensitive to ISO and HAL (Fig 5D, S4G Fig; Table 1).

Parietal association cortex (PAC)

The CMT and DMT neurons send major projections into the posterior PAC (Allen Mouse Brain Connectivity Database) [28]. The PAC is involved in episodic memory retrieval, spatial

Vestibular Nucleus (VN)
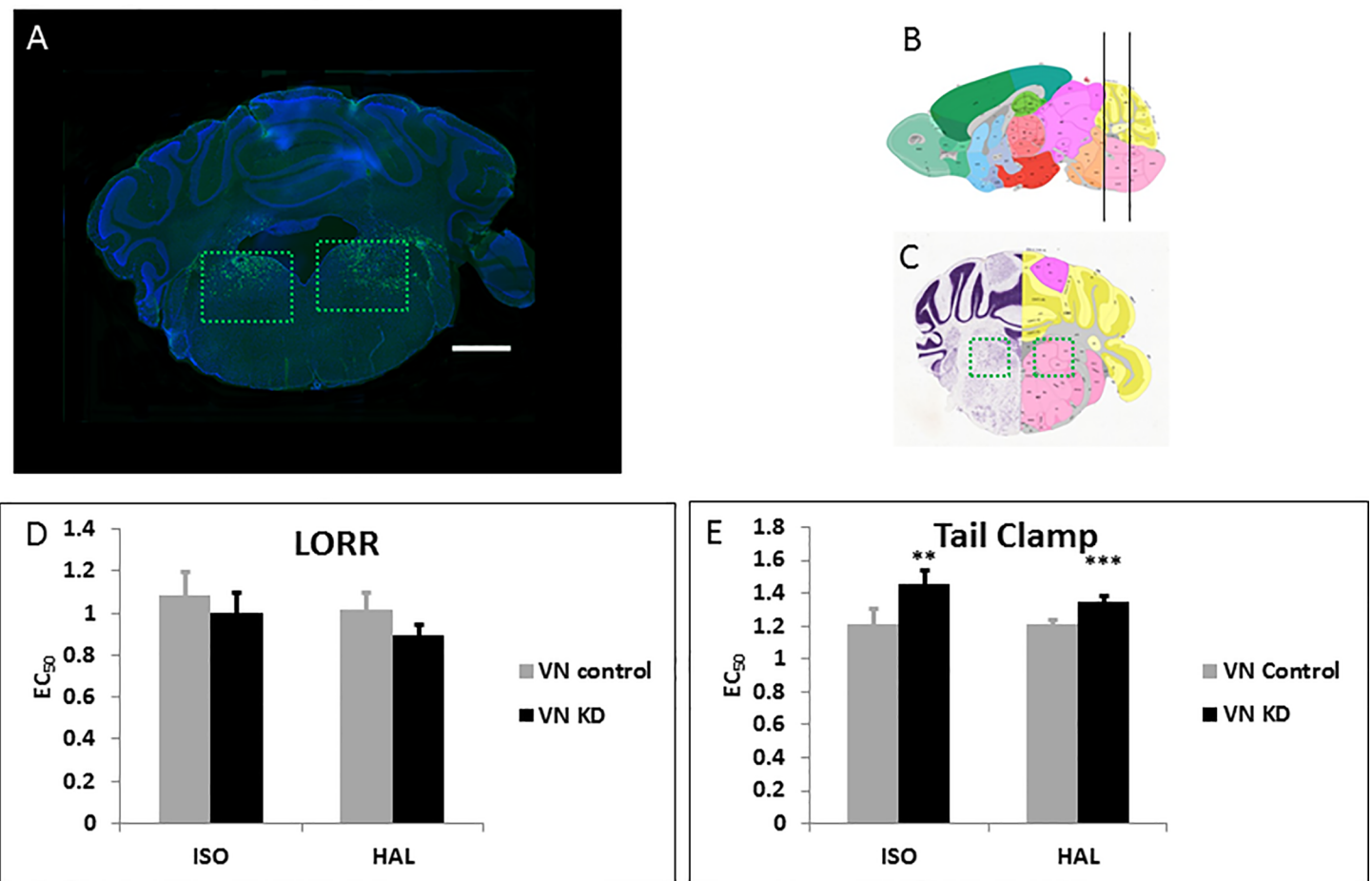
Fig 2. Knockdown of *Ndufs4* in the VN. A. Fluorescent images of brain slices from mice injected with active WT-Cre virus into the VN (Coordinates: ML = ± 1.25; AP = -5.8; DV = 4.3, Magnification X40). Virus-infected cells appear green due to the viral GFP co-expression B, **C.** Schematic figures from the Allen mouse brain atlas [24] (Image credit: Allen Institute) depicting the antero-posterior (**B**), mediolateral (**C**) and dorso-ventral (**C**) viral spread (green boxed regions in **C**). Reprinted from the Allen mouse brain atlas under a CC BY license, with permission from the Allen Institute, original copyright 2008. **D.** EC$_{50}$s for ISO and HAL for the active (n = 7, black bars) and sham (n = 6, grey bars) virus injected mice in the LORR assay. **E.** EC$_{50}$s for ISO and HAL for the active (n = 7, black bars) and sham (n = 6, grey bars) virus injected mice in the TC assay. Scale bar: 1mm. **indicates p-values <0.005, *** indicates p-values <0.001. The error bars in all bar graphs indicate standard deviation.

https://doi.org/10.1371/journal.pone.0188087.g002

Table 1. EC$_{50}$s for ISO and HAL for the WT-Cre and Δ-Cre virus-injected mice in the LORR and TC assays.

Type of injection	Region injected	Behavioral test	EC$_{50}$ ISO (SD)	EC$_{50}$ HAL (SD)	N (Gender)
AAV-WT-Cre-GFP	VN	LORR	1.00 (0.09)	0.90 (0.05)	7 (4F/3M)
AAV-Δ-Cre-GFP	VN	LORR	1.1 (0.1)	1.02 (0.08)	6 (4F/2M)
AAV-WT-Cre-GFP	VN	TC	1.45 (0.09)* $p = 0.002$	1.35 (0.04)* $p = 3.6 \times 10^{-5}$	7 (4F/3M)
AAV-Δ-Cre-GFP	VN	TC	1.2 (0.1)	1.21 (0.02)	6 (4F/2M)
AAV-WT-Cre-GFP	MPTA	LORR	0.79 (0.06)* $p = 0.01$	0.82 (0.06)	6 (3F/3M)
AAV-Δ-Cre-GFP	MPTA	LORR	0.90 (0.07)	0.87 (0.04)	7 (3F/4M)
AAV-WT-Cre-GFP	MPTA	TC	1.1 (0.2)	1.1 (0.1)	6 (3F/3M)
AAV-Δ-Cre-GFP	MPTA	TC	1.25 (0.05)	1.23 (0.09)	7 (3F/4M)
AAV-WT-Cre-GFP	CMT	LORR	0.80 (0.07)* $p = 0.003$	0.77 (0.07)* $p = 0.004$	6 (4F/2M)
AAV-Δ-Cre-GFP	CMT	LORR	1.0 (0.1)	1.0 (0.1)	6 (2F/4M)
AAV-WT-Cre-GFP	CMT	TC	1.0 (0.1)* $p = 0.008$	1.02 (0.08)* $p = 3.4 \times 10^{-5}$	6 (4F/2M)
AAV-Δ-Cre-GFP	CMT	TC	1.2 (0.1)	1.31 (0.08)	6 (2F/4M)
AAV-WT-Cre-GFP	DMT	LORR	0.80 (0.03)* $p = 0.001$	0.74 (0.02)* $p = 3.8 \times 10^{-7}$	6 (4F/2M)
AAV-Δ-Cre-GFP	DMT	LORR	0.93 (0.04)	1.02 (0.05)	6 (2F/4M)
AAV-WT-Cre-GFP	DMT	TC	0.92 (0.09)* $p = 0.0004$	0.87 (0.04)* $p = 1.2 \times 10^{-7}$	6 (4F/2M)
AAV-Δ-Cre-GFP	DMT	TC	1.2 (0.1)	1.33 (0.07)	6 (2F/4M)
AAV-WT-Cre-GFP	PAC	LORR	0.71 (0.05)* $p = 3.5 \times 10^{-7}$	0.68 (0.06)* $p = 0.0001$	6 (1F/5M)
AAV-Δ-Cre-GFP	PAC	LORR	0.95 (0.02)	1.0 (0.1)	6 (3F/3M)
AAV-WT-Cre-GFP	PAC	TC	0.85 (0.05)* $p = 9.4 \times 10^{-8}$	0.77 (0.09)* $p = 5.4 \times 10^{-7}$	6 (1F/5M)
AAV-Δ-Cre-GFP	PAC	TC	1.21 (0.06)	1.23 (0.07)	6 (3F/3M)

* indicates p-values < 0.01. p values listed compare region specific KO EC$_{50}$s to control animals injected with sham Cre.

reasoning, perception and attention. We surmised that glutamatergic relaying to the cortex might be compromised in the regional knockdown, leading to hypersensitivity to anesthetics. We therefore injected the WT-Cre (Fig 6A, 6B and 6C) and Δ-Cre (S3E Fig) viruses bilaterally into the PAC. Knock down of *Ndufs4* in the PAC caused the highest level of hypersensitivity recorded in our study for both ISO and HAL for TC (Fig 6E, S4J Fig; Table 1). For LORR, knockdown of *Ndufs4* in the PAC caused hypersensitivity to ISO and HAL (EC$_{50}$(control) 1.0 ±0.1%, EC$_{50}$(KD) 0.68±0.06%; p = 0.0001) (Fig 6D, S4I Fig; Table 1).

Brightly fluorescing cells also appeared in the central thalamus of the brains of mice injected with the Δ−Cre and WT-Cre viruses (Fig 7) into the PAC. This provides evidence of antero-grade transmission of the GFP signal from the PAC to the thalamus and for the existence of a thalamocortical circuit possibly involved in mediating the anesthetic sensitivity of the *Ndufs4 (KO)* mice [3]. To determine whether the excitatory neurotransmission in the PAC circuit is compromised by *Ndufs4* mutation, we recorded the field excitatory postsynaptic potentials (fEPSPs) in the PAC of sagittal brain slices of *Ndufs4(KO)* and control sibling mice (Fig 8). The amplitudes of fEPSPs in the PAC were significantly decreased during 0.6% ISO exposure (cor-responds to 248 µM at room temperature) in the *Ndufs4(KO)* when compared to the control slices (p = 0.00008). There was a trend for decrease in the fiber volley amplitude of the global

Mesopontine Tegmental Anesthetic Area (MPTA)
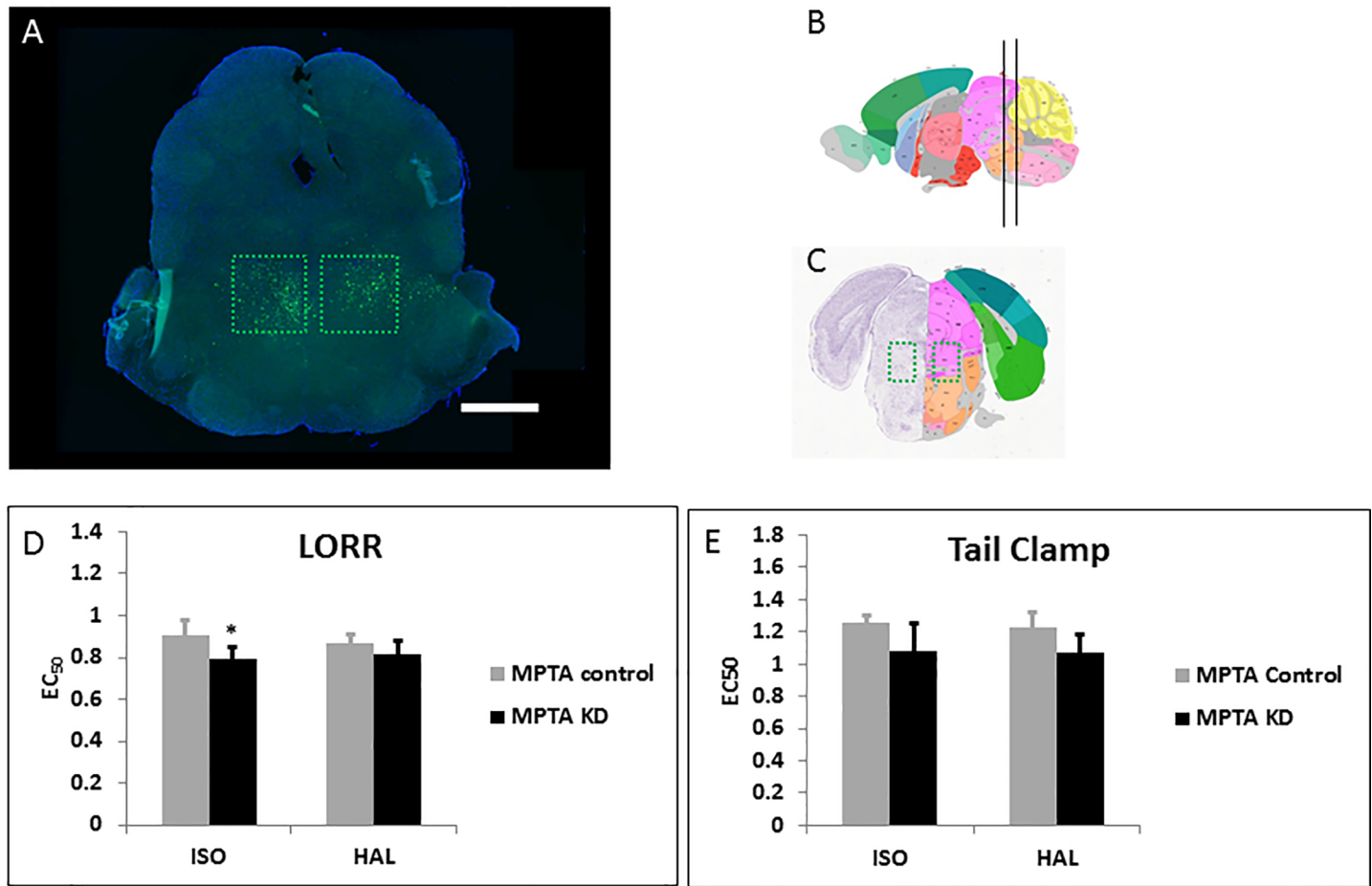
Fig 3. Knockdown of *Ndufs4* in the MPTA. A. Fluorescent images of brain slices from mice injected with active WT-Cre virus (**A**) into the MPTA (Coordinates: ML = ± 0.70; AP = -4.6; DV = 4.1, Magnification X40). **B**, **C.** Schematic figures from the Allen mouse brain atlas [24] depicting the viral spread (Image credit: Allen Institute). Reprinted from the Allen mouse brain atlas under a CC BY license, with permission from the Allen Institute, original copyright 2008. **D.** EC_{50}s for ISO and HAL for the active (n = 6, black bars) and sham (n = 7, grey bars) virus injected mice in the LORR assay. **E.** EC_{50}s for ISO and HAL for the active (n = 6, black bars) and sham (n = 7, grey bars) virus injected mice in the TC assay. Scale bar: 1mm. **indicates p-value <0.01.

https://doi.org/10.1371/journal.pone.0188087.g003

KO brain slices during 0.6% ISO exposure when compared to the control brain slices, however the change did not reach statistical significance (p = 0.015).

Discussion

Inactivation of a complex I subunit in the thalamocortical circuit caused striking VA hypersensitivity to both the LORR and TC responses. The degrees of change are especially noteworthy given that inactivation specifically knocked down levels of the protein only in very confined regions of the CNS, after development was largely completed. Acute local inactivation of a mitochondrial gene in an otherwise wild type mouse minimizes compensatory developmental changes or latent nonspecific CNS degeneration seen in the global KO, as potential confounders of data interpretation. Although we did not measure mitochondrial function in these microscopic regions of the brain, we infer that complex I function is defective in the regions where *Ndufs4* is knocked down. In turn, we interpret these data to indicate that anesthetic hypersensitivity here results specifically from acute mitochondrial dysfunction. The simplest

Central Medial Thalamus (CMT)
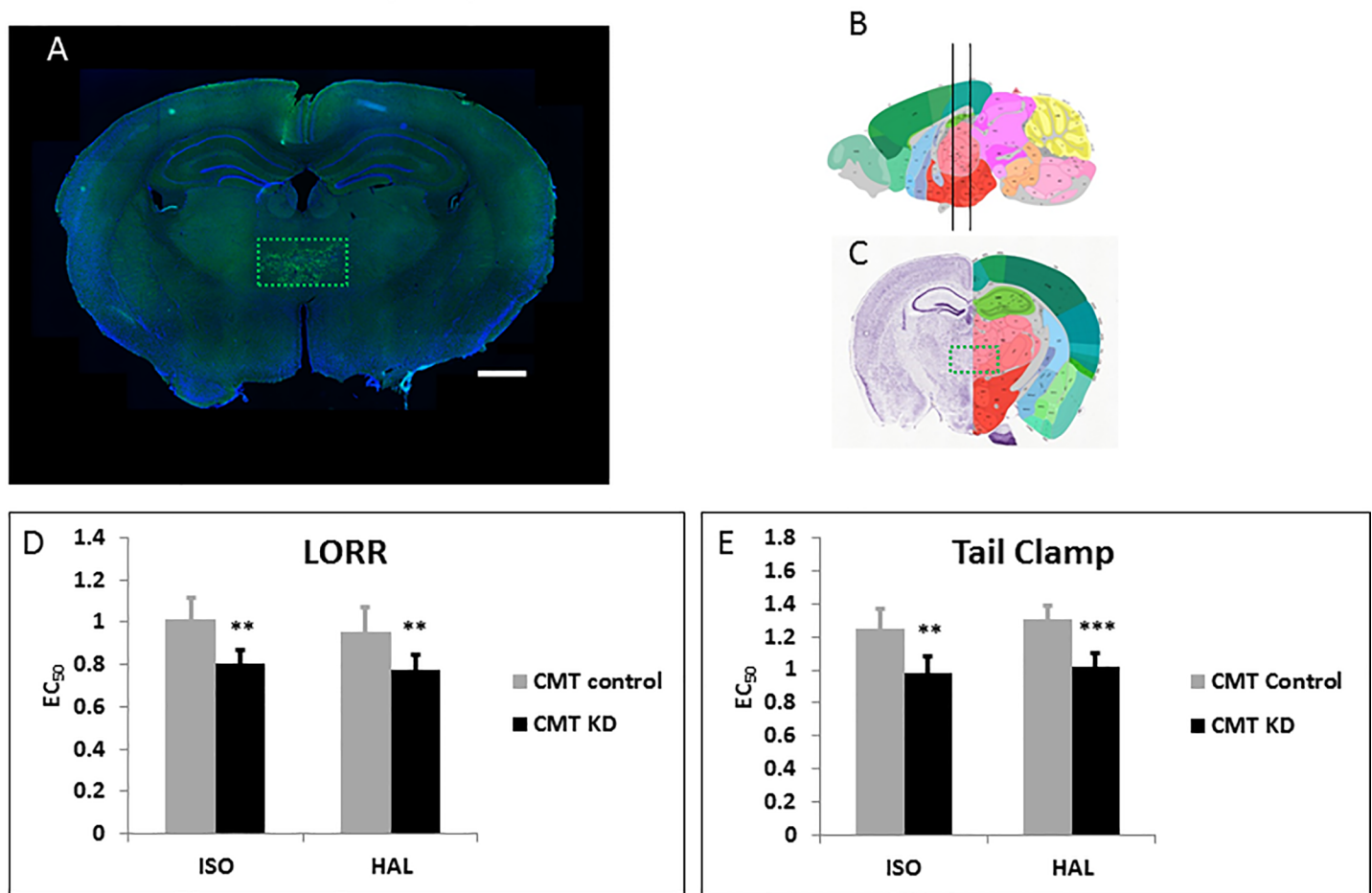
Fig 4. Knockdown of *Ndufs4* in the CMT. A. Fluorescent images of brain slices from mice injected with active WT-Cre virus (**A**) into the CMT (Co-ordinates: ML = ± 0.32; AP = -1.2; DV = 3.85, Magnification X40). **B**, **C.** Schematic figures from the Allen mouse brain atlas [24] depicting the viral spread (Image credit: Allen Institute). Reprinted from the Allen mouse brain atlas under a CC BY license, with permission from the Allen Institute, original copyright 2008. **D.** EC_{50}s for ISO and HAL for the active (n = 6, black bars) and sham (n = 6, grey bars) virus injected mice in the LORR assay. **E.** EC_{50}s for ISO and HAL for the active (n = 6, black bars) and sham (n = 6, grey bars) virus injected mice in the TC assay. Scale bar: 1mm. **indicates p-values <0.005, *** indicates p-values <0.001.

https://doi.org/10.1371/journal.pone.0188087.g004

explanation of our data is that VAs directly inhibit complex I function [29]; the resulting region-specific decrease in metabolism leads to the anesthetized state.

Regional metabolism is certainly altered in the CNS while anesthetized, but this may result from or cause the anesthetized state [19, 25, 30]. However, we know that defects in mitochondrial complex I increase anesthetic sensitivity without known changes in ion channel characteristics [9]. In addition, the EC_{50} of the *Ndufs4(KO)* mutant, 0.4% isoflurane, is well below the concentration that produces significant effects in putative VA targets that may reduce regional metabolism as a secondary effect. Given that complex I dysfunction profoundly sensitizes worms, mice and children to VAs [1–3, 31], this effect appears highly conserved across the animal kingdom.

Mitochondrial function represents a key component of normal CNS metabolism, since oxidative phosphorylation is necessary for synaptic function [32, 33]. Complex I is the rate limiting step of electron transport [34, 35]; isolated mitochondria from the *Ndufs4(KO)* brain display significantly reduced Complex I activity [7]. Prior hypotheses suggested a generalized

Dorsal Medial Thalamus (DMT)
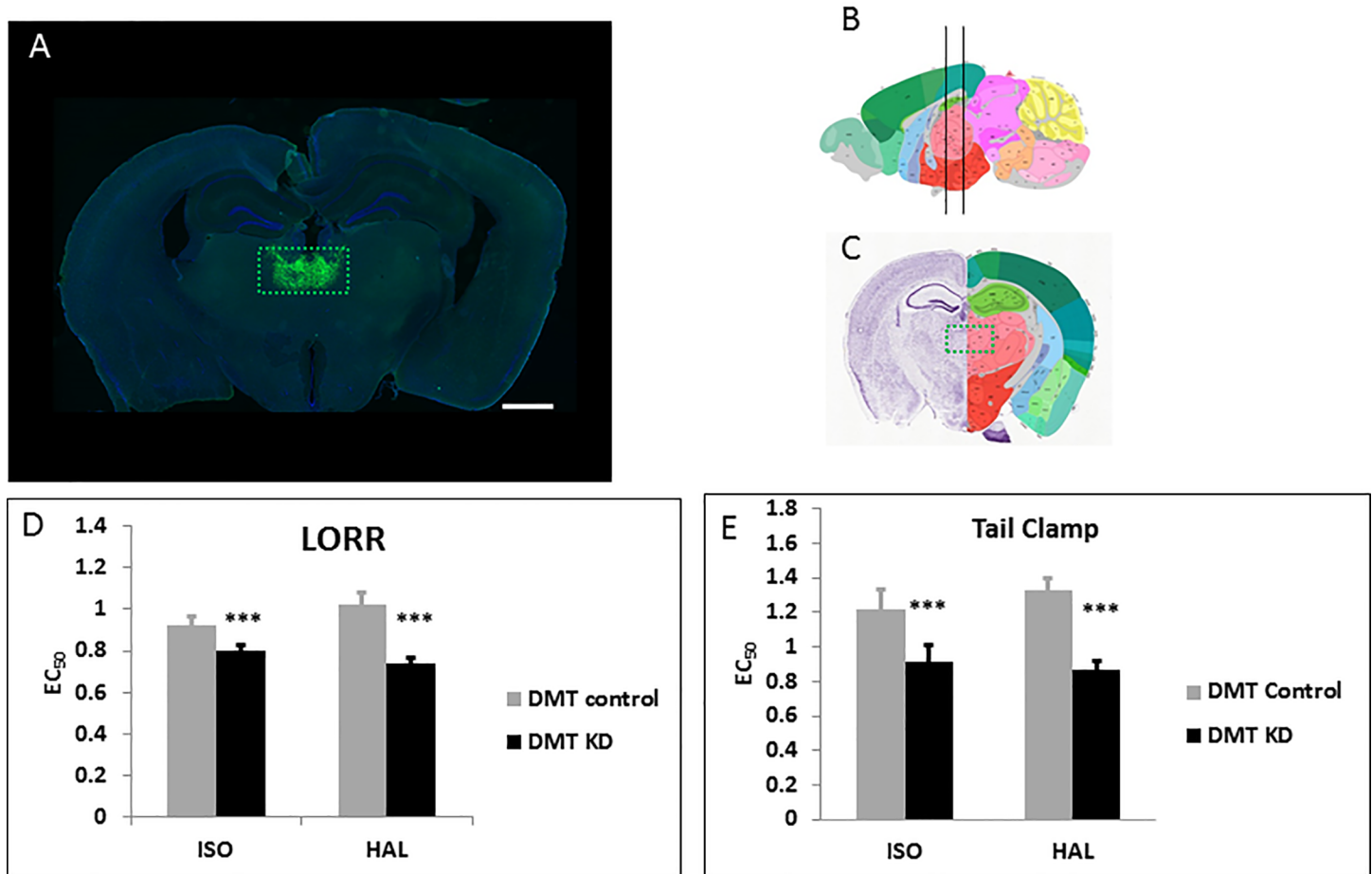
Fig 5. Knockdown of *Ndufs4* in the DMT. A. Fluorescent images of brain slices from mice injected with active WT-Cre virus (**A**) into the DMT (Co-ordinates: ML = ± 0.32; AP = -1.2; DV = 3.7, Magnification X40). **B, C.** Schematic figures from the Allen mouse brain atlas [24] depicting the viral spread (Image credit: Allen Institute). Reprinted from the Allen mouse brain atlas under a CC BY license, with permission from the Allen Institute, original copyright 2008. **D.** EC_{50}s for ISO and HAL for the active (n = 6, black bars) and sham (n = 6, grey bars) virus injected mice in the LORR assay. **E.** EC_{50}s for ISO and HAL for the active (n = 6, black bars) and sham (n = 6, grey bars) virus injected mice in the TC assay. Scale bar: 1mm. *** indicates p-values <0.001.

https://doi.org/10.1371/journal.pone.0188087.g005

decrease in neuronal activity as a mechanism of anesthesia [10, 12]. However, recent work indicates that localized CNS effects may underlie the anesthetic state and multiple regions have been suggested as mediating these effects [14, 19, 30, 36, 37]. The data presented here highlight the probable importance of normal mitochondrial function within very circumscribed key regions of the brain that are necessary to support normal response to anesthetics. The anesthetic inhibition of response to TC is thought to result from effects on the spinal cord with some supraspinal modification [18, 38]. The LORR is used as a surrogate for unconsciousness [39, 40]. Our results demonstrate different phenotypes for these endpoints mediated by mitochondrial dysfunction in various regions of the brain. We discuss LORR and TC separately below.

Loss of righting reflex

It is known that the thalamus displays suppressed metabolism [19] and decreased synaptic activity during anesthesia [37, 41]. The hypersensitivity seen in our animals after viral injection

Parietal Association Cortex (PAC)
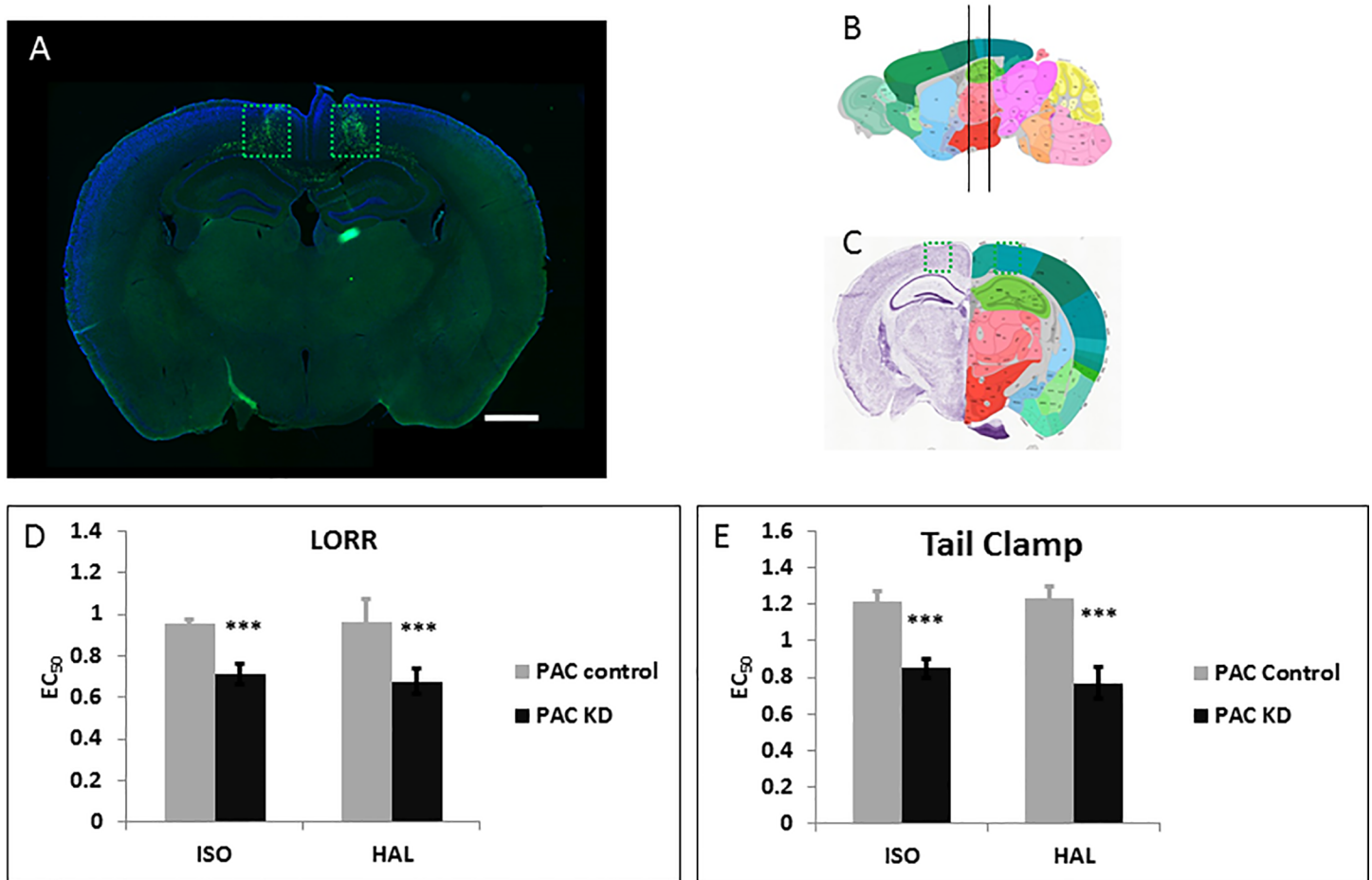
Fig 6. Knockdown of *Ndufs4* in the PAC. A. Fluorescent images of brain slices from mice injected with active WT-Cre virus (**A**) into the PAC (Co-ordinates: ML = ± 0.80; AP = -1.75; DV = 0.9, Magnification X40). **B**, **C.** Schematic figures from the Allen mouse brain atlas [24] depicting the viral spread (Image credit: Allen Institute). Reprinted from the Allen mouse brain atlas under a CC BY license, with permission from the Allen Institute, original copyright 2008. **D.** EC_{50}s for ISO and HAL for the active (n = 5, black bars) and sham (n = 6, grey bars) virus injected mice in the LORR assay. **E.** EC_{50}s for ISO and HAL for the active (n = 5, black bars) and sham (n = 6, grey bars) virus injected mice in the TC assay. Scale bar: 1mm. *** indicates p-values <0.001.

into the medial thalamus corroborates a role for the medial thalamic nuclei in determining anesthetic sensitivity for LORR. Our results support electrophysiologic work showing thalamocortical activity correlated with anesthetic depth [42]. Since the medial thalamus relays glutamatergic signals to the cortex [43, 44], VAs likely exert their effects through suppression of these pathways. The mouse connectivity database of the Allen Institute also shows projections from the central medial thalamus populating the parietal association cortex [28, 45]. We have confirmed a circuit between the PAC and the thalamus, with reciprocal projections from the PAC to the thalamus. Viral inactivation of *Ndufs4* in the PAC reveals that this region contributes about 1/2 of the hypersensitivity displayed by the whole body *Ndufs4(KO)* for ISO and HAL in the LORR assay (Table 1).

The reduced fEPSP amplitudes in the PAC of *Ndufs4* global KO during 0.6% ISO exposure likely contributes to the increased VA sensitivity seen in the global KO. This is consistent with studies demonstrating that dexmedetomidine induced loss of consciousness in healthy volunteers preferentially decreased cerebral glucose metabolic rate and blood flow in thalamus and
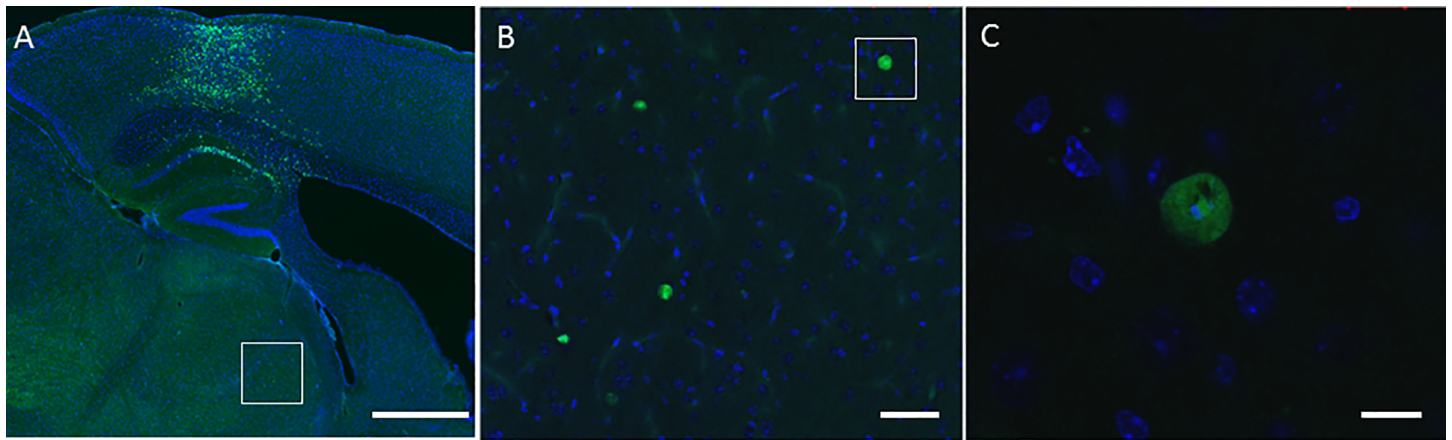
Fig 7. The thalamocortical circuit. A. Fluorescent image of a brain slice from a mouse injected with Δ-Cre virus into the PAC (Magnification X40). **B.** Magnified confocal image of the white-boxed region within the thalamus in **A** (Magnification X200). **C.** Magnified confocal image of white boxed region in **B** showing viral-GFP expressing cells in the thalamus following injection into the PAC (Magnification X1000). Scale bars: A-1mm, B-50μm, C-10μm.

https://doi.org/10.1371/journal.pone.0188087.g007

in an area corresponding to the PAC of mice [19]. While the functional connectivity within cortical regions was preserved, connectivity between medial thalamus and the cortical regions was disrupted during the unconscious state and re-established during regain of consciousness. This same area, part of a larger region called the DMN (default mode network) in humans [46], shows a direct correlation between connectivity within the DMN and levels of consciousness in patients with disorders of consciousness [47, 48]. We conclude that the thalamocortical sensory relaying is bioenergetically demanding and sensitive to mitochondrial inhibition by VAs.

Studies by Devor and colleagues in rats have shown that the mesopontine tegmental anesthetic area (MPTA) is important for mediating anesthetic LORR sensitivity to pentobarbital [17]. However, we found MPTA KD mice were mildly hypersensitive only to ISO for LORR. It is possible that our injections did not localize to the MPTA, or the precise location of the MPTA may differ between the rat and mouse brain. It is also possible that the MPTA is not an important region for mediating the anesthetic sensitivity of HAL, or that the mitochondrial mutation mediates anesthetic hypersensitivity by exerting regional effects elsewhere.

Tail clamp

Similar to the effects on LORR, *Ndufs4* loss in the CMT/DMT and PAC accounts for approximately half of the hypersensitivity displayed by the whole body KO for ISO and HAL in the TC assay [3]. The ascending spinal cord and the ventro-posterior brain stem nuclei of the primary somatic pathways transmit nociceptive signals from the peripheral nervous system to the somatosensory, the parieto-insular and the anterior cingulate cortices resulting in pain perception [49, 50]. The medial thalamus is involved in the medial pain perception pathway and is suppressed by pentobarbital during noxious stimulation [27]. The DMT also drives feed forward inhibition of the anterior cingulate cortex to limit excitatory input processing and firing of cortical neurons, resulting in better temporal precision of the circuit [51]. Similar to the effects on LORR, we propose that mitochondrial dysfunction disrupts the temporal fidelity within the thalamocortical circuits such that the pain perception pathway is inhibited more completely by ISO and HAL when mitochondrial dysfunction is present prior to anesthetic exposure.

It is interesting that VN-specific *Ndufs4* KD caused resistance to VAs in the tail clamp assay. In contrast to the role played by the cortex in central pain perception, the higher brain
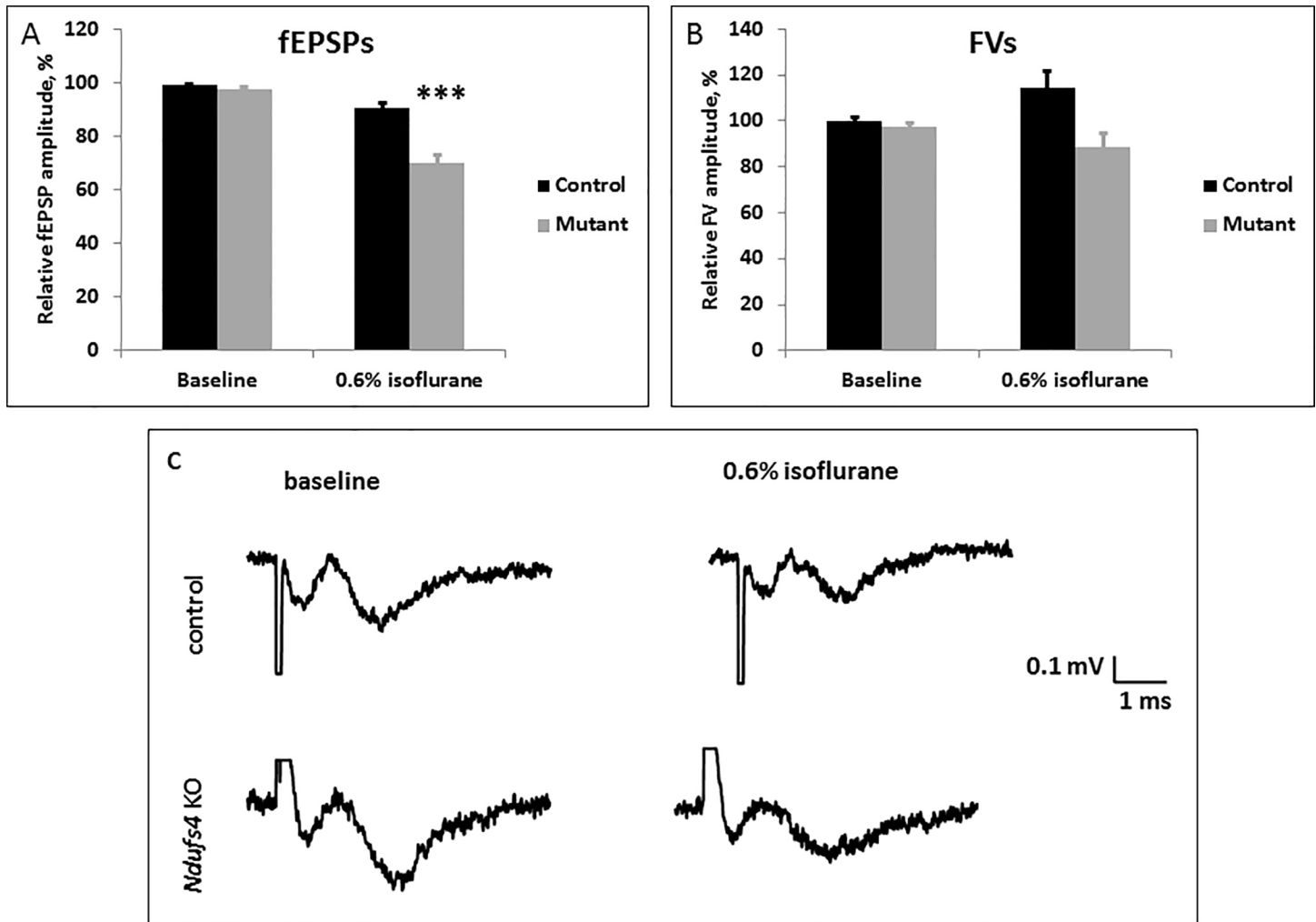
Fig 8. Electrophysiological field recordings of the excitatory synaptic transmission. A. Amplitudes of fEPSPs decreased with 0.6% (248 µM) ISO exposure in control and *Ndufs4(KO)* brain slices. The decrease of fEPSPs was significantly greater for the *Ndufs4(KO)* than the control (*** indicates p-value <0.001). **B.** Fiber volleys of both genotypes were not significantly affected by the isoflurane exposure. **C.** Representative traces of field recordings from control and KO slices before and during exposure to 0.6% ISO (equivalent to 248 µM). 0.6% ISO exposure led to a significantly larger decrease in the amplitudes of fEPSP in the KO when compared to the respective decrease in controls. The amplitudes of the fiber volleys were decreased (statistically tending to significance, $p = 0.015$) by 0.6% ISO exposure in both genotypes.

centers have also been shown to modulate nociceptive transmission so that spinal transection increases nociceptive reflexes [52]. The descending spinal cord modulatory effects by the higher brain centers could be facilitating or inhibitory [53, 54]. Antognini *et al.* showed that preferential anesthetization of the goat brain bypassing the spinal cord increased the isoflurane requirement to inhibit the sensitivity to dew-claw stimulation [18]. Rampil *et al.* showed that depression of the spinal motor neurons may contribute to the lack of response to painful stimuli mediated by various inhalational anesthetics in rats [55, 56]. Our results are most consistent with descending inhibitory signaling through the VN to the spinal cord being decreased by the *Ndufs4(KO)*.

We propose that the excitatory thalamocortical firing to the PAC mediates both consciousness and nociception. The posterior brain stem acts as a switch between nociception, during which excitatory cortical firing to the brain stem dominates, and antinociception, during

which inhibitory cortical firing to the VN and the downstream spinal neurons dominates. Supporting the model, glucose uptake [57] and c-FOS staining [58] in the VN increased during isoflurane anesthesia, indicating that the anesthetized state may require increased energy production in the VN which is rendered inadequate by the mitochondrial mutation.

Conclusion

We report the first demonstration linking regional CNS inactivation of a mitochondrial protein to sensitivity to volatile anesthetics. We infer that localized knockdown of NDUFS4 results in a regional defect in mitochondrial respiration as is seen in the global KO. Mitochondria therefore represent a putative novel target for volatile anesthetics. Restriction of mitochondrial defects to the thalamocortical circuit causes greater than half of the change in anesthetic sensitivities seen in the total loss of the *Ndufs4* gene. Regional bioenergetic capacities and mitochondrial function are likely an important determinant of response to volatile anesthetics, and may underlie the mechanism of action of volatile anesthetics.

Materials and methods

Animal maintenance

All studies were approved by the Animal Care and Use Committee of the Seattle Children's Research Institute. Mice were maintained on standard rodent diet at 22˚C with 12-hour dark/light cycles. *Ndufs4*lox/lox mice with a mixed 129/Sv:C57Bl/6 genetic background [6] were a kind gift from Richard Palmiter (Howard Hughes Medical Institute and the University of Washington, Seattle, WA).

Intracranial virus delivery

The adeno-associated viruses rAAV/WT-Cre GFP and the rAAV/Delta(Δ)-Cre GFP viruses [59, 60] were purchased from UNC Vector Core (Chapel Hill, NC) and diluted in PBS at a titer of 2×10^9 viral genomes/μl. These viruses encode wild-type active Cre-recombinase (WT-Cre, active) or mutated defective Cre-recombinase (Δ-Cre, control) respectively and green fluorescent protein (GFP) and are known to be taken up by all types of cells in the injected region [61]. Delivery of active Cre expressing AAV to the various regions of *Ndufs4*lox/lox mice brains created region-specific loss of the protein NDUFS4. Male and female animals aged between 35 to 40 days of age were anesthetized with isoflurane and either virus was injected into various brain regions using the motorized Robot stereotax (Neurostar GmbH, Tubingen, Germany) as per manufacturer instructions. Briefly, the anesthetized mouse was attached to the stereotax with inline isoflurane (induction with 5% ISO and maintenance with 1.5% ISO) delivered through a face mask. An incision was made on the shaved and sterilized supracranial skin exposing the skull. Either virus was injected using a motorized injector after drilling holes in the cranium at stereotaxically defined bilateral locations. The quantities and co-ordinates of the viral injections are listed in S2 Table. For VN, CMT, DMT and PAC, coordinates were used from the Allen Brain Atlas. The location of the MPTA was approximated by using rat coordinates. The mice were allowed to recover for 3 weeks before behavioral testing using halothane (HAL) or isoflurane (ISO).

Behavioral testing

Mice were anesthetized with ISO or HAL and assayed for LORR or response to TC as described by Sonner *et al*. [62] and the anesthetic concentrations analyzed by gas chromatography [63]. The EC$_{50}$s for loss of response to TC were used as the equivalent of minimum

anesthetic concentrations (MAC) for loss of nociceptive motor response. The EC_{50}s for the loss of righting reflex were used as a measure of the consciousness status of the animal. Animals were kept warm on a heating pad throughout and allowed to recover for at least 24 h between behavioral assays. Each animal underwent TC and LORR testing in a randomized order. No significant differences were noted between the anesthetic sensitivity of the subjected mice due to prior anesthetic exposure during the randomized tests. The EC_{50} for an anesthetic was the average of the concentrations for induction (defined as the average concentrations of gas in the last sample before loss of response and in the first sample at which the response was lost) and emergence (defined as the average concentration of gas in the first sample at which the animal once again responded, and the sample immediately prior). Mice were tested at 3 weeks after virus injection for both behavioral endpoints in both anesthetics. All animals survived the anesthetic exposures. They were then sacrificed for immunohistochemical analyses at 28 days after injection.

Histopathological analyses

Mice were euthanized using CO_2, and brains were fixed in cold 4% paraformaldehyde, post-fixed overnight at 4°C, cryoprotected in 30% sucrose-PBS for three days and embedded in optimal cutting temperature compound (OCT). Brains were then sliced at 30 μm thickness and serial slices were collected in PBS in 24-well dishes. Slices at 180μm intervals were selected and mounted on glass slides, analyzed and imaged under a fluorescence microscope (upright Zeiss Axioskop equipped with an Attoarc 100W HBO lamp, an Axiocam color charge-coupled device camera (type 412–312) and Axiovision v3.1 software) to assess the viral spread of infection. For heat-induced epitope retrieval, captured slices on glass slides were boiled in 10mM sodium citrate buffer (pH 6.0) at 100°C for 20 minutes using a water bath [64]. Slides were then blocked in PBS with 10% normal donkey serum overnight at 4°C. Primary antibodies, mouse anti-NDUFS4 (Santa Cruz; dilution 1:50), mouse anti-cytochrome C (MitoSciences; dilution 1:300) and goat anti-*GFP* (Abcam; dilution 1:200) were incubated overnight at 4°C. Secondary antibodies, rabbit anti-mouse Alexa Fluor 568 (Life Technologies; dilution 1:2000) and donkey anti-goat AlexaFluor 488 (Life Technologies; dilution 1:2000) were incubated for one hour at RT. After mounting the slices in DAPI Fluoromount-G solution (Southern Biotech), they were imaged by confocal microscopy (Zeiss LSM 710 Imager Z2 laser scanning confocal microscope, Zen 2009 software). To assess the efficiency of the AAV-mediated knockdown, Alexa Fluor 568 tagged NDUFS4 expression (red immunofluorescence) was quantified in the virus infected cells which co-expressed the Green Fluorescent Protein (GFP, Alexa Fluor 488 tagged, green immunofluorescence), and expressed as a percentage of total infected cells. 20 image fields were quantified per injected locus. These were from 5 bilateral alternating slices, 4 image fields per slice, of 85μmX85μm size each, quantified by a blinded scorer.

Field potential recordings

Field potential experiments were performed as described previously with modifications [9]. Briefly, 400 μm thick sagittal slices of the mouse brain were collected. The recording electrode was placed in parietal association cortex and the stimulation electrode was positioned ~1mm rostrally in the cortex. The amplitude was selected to produce half-maximal fEPSP amplitude. The stimulus duration was 100 μs. Field potential signals were amplified using EPC10 amplifier (HEKA) and digitized with Digidata 1322A (Axon Instruments) at 250 kHz sampling rate. Stimulations were applied at 0.033 Hz. Isoflurane was applied in the superfusate at equilibrated concentrations delivered by passing carbogen through a calibrated isoflurane

vaporizer (Scivena Scientific TEC-3 and Patterson Veterinary TEC-3). Amplitudes of fEPSPs and FVs were normalized to their respective averages during the last 5 min prior to isoflurane exposure for each individual recording.

Statistical analyses

A statistical power analysis was performed using the control values and standard deviation for the uninjected control mice as reference. Specifying an effect size of 0.25, α of 0.05 and power of 0.8 for each assay (LORR-ISO, LORR-HAL, TC-ISO and TC-HAL), we found the minimal sample size to be 2. For all region-specific injections, we used a minimal cohort size of 6 per category. The effective concentration for 50% of the animals tested (EC_{50}) for each volatile anesthetic was determined as described by Sonner *et al.* [62], using an up and down method. Values for EC_{50}s were compared between the WT and regional KD strains by Student's t-test using GraphPad Prism®. For the electrophysiological field recordings, values for fEPSPs and fiber volleys for slices (n = 7 for control, n = 6 for *Ndufs4(KO)*) were averaged and significance analyzed by one-way ANOVA using GraphPad Prism®. Significance was defined as a p<0.01.

Supporting information

S1 Fig. Loss of NDUFS4 in the PAC. Unmerged and merged confocal images of the (A) Δ–Cre injected and (B) WT-Cre injected PAC (Magnification X1000). White arrows point to cells which retained the red NDUFS4 fluorescence in the absence of virus infection. Scale bar: 10μm.
(TIF)

S2 Fig. Cytochrome C immunostaining in the virus injected regions. Unmerged and merged confocal images of the (A) Δ–Cre injected and (B) WT-Cre injected VN (Magnification X1000).
(TIF)

S3 Fig. Fluorescent images of brain slices from mice injected with inactive Δ-Cre virus into the (A) VN, (B) MPTA, (C) CMT, (D) DMT and (E) PAC (Magnification X40). Scale bar: 1mm.
(TIF)

S4 Fig. Scatter plots showing individual EC_{50} values using ISO and HAL for LORR and TC in the vestibular nucleus (VN), mesopontine tegmental anesthetic area (MPTA), central medial thalamus (CMT), dorsal medial thalamus (DMT) and parietal association cortex (PAC). Large cross bars represent the mean of EC_{50}s for ISO (red dots) and HAL (black dots) for the WT-Cre (KD) and Δ-Cre (Control) virus-injected mice in the LORR and TC assays. Small crossbars represent the standard error of the mean. Plots depict viral injections performed into the VN (**A & B**, Control n = 6, KD n = 7), MPTA (**C & D**, Control n = 7, KD n = 6), CMT (**E & F**, n = 6 for Control and KD), DMT (**G & H**, n = 6 for Control and KD) and PAC (**I & J**, n = 6 for Control and KD).
(TIF)

S1 Table. EC_{50}s for ISO and HAL for the the global KO and control mice in the LORR assay. Previously published data for the TC assay [3] are included for comparison.
(DOC)

S2 Table. Viral injection coordinates and quantities.
(DOC)

Acknowledgments

Author Contributions

Conceptualization: Renjini Ramadasan-Nair, Leslie S. Itsara, Philip G. Morgan, Margaret M. Sedensky.

Data curation: Renjini Ramadasan-Nair, Jessica Hui, Pavel I. Zimin, Leslie S. Itsara.

Formal analysis: Renjini Ramadasan-Nair, Jessica Hui, Pavel I. Zimin, Leslie S. Itsara.

Funding acquisition: Philip G. Morgan, Margaret M. Sedensky.

Investigation: Renjini Ramadasan-Nair, Jessica Hui, Pavel I. Zimin, Leslie S. Itsara, Philip G. Morgan, Margaret M. Sedensky.

Methodology: Renjini Ramadasan-Nair, Pavel I. Zimin, Leslie S. Itsara, Philip G. Morgan, Margaret M. Sedensky.

Project administration: Renjini Ramadasan-Nair, Philip G. Morgan, Margaret M. Sedensky.

Resources: Renjini Ramadasan-Nair, Philip G. Morgan, Margaret M. Sedensky.

Software: Renjini Ramadasan-Nair.

Supervision: Renjini Ramadasan-Nair, Philip G. Morgan, Margaret M. Sedensky.

Validation: Renjini Ramadasan-Nair, Jessica Hui, Pavel I. Zimin, Leslie S. Itsara, Margaret M. Sedensky.

Visualization: Renjini Ramadasan-Nair.

Writing – original draft: Renjini Ramadasan-Nair, Philip G. Morgan, Margaret M. Sedensky.

Writing – review & editing: Renjini Ramadasan-Nair, Philip G. Morgan, Margaret M. Sedensky.

References

1. Kayser EB, Morgan PG, Sedensky MM. GAS-1: a mitochondrial protein controls sensitivity to volatile anesthetics in the nematode Caenorhabditis elegans. Anesthesiology. 1999; 90(2):545–54. Epub 1999/ 02/10. PMID: 9952163.

2. Morgan PG, Hoppel CL, Sedensky MM. Mitochondrial defects and anesthetic sensitivity. Anesthesiology. 2002; 96(5):1268–70. PMID: 11981173.

3. Quintana A, Morgan PG, Kruse SE, Palmiter RD, Sedensky MM. Altered anesthetic sensitivity of mice lacking Ndufs4, a subunit of mitochondrial complex I. PLoS One. 2012; 7(8):e42904. Epub 2012/08/23. https://doi.org/10.1371/journal.pone.0042904 PMID: 22912761; PubMed Central PMCID: PMC3422219.

4. Cohen PJ. Effect of anesthetics on mitochondrial function. Anesthesiology. 1973; 39(2):153–64. Epub 1973/08/01. PMID: 4146381.

5. Harris RA, Munroe J, Farmer B, Kim KC, Jenkins P. Action of halothane upon mitochondrial respiration. Arch Biochem Biophys. 1971; 142(2):435–44. Epub 1971/02/01. PMID: 4396285.

6. Kruse SE, Watt WC, Marcinek DJ, Kapur RP, Schenkman KA, Palmiter RD. Mice with mitochondrial complex I deficiency develop a fatal encephalomyopathy. Cell Metab. 2008; 7(4):312–20. Epub 2008/ 04/09. https://doi.org/10.1016/j.cmet.2008.02.004 PMID: 18396137; PubMed Central PMCID: PMC2593686.

7. Johnson SC, Yanos ME, Kayser EB, Quintana A, Sangesland M, Castanza A, et al. mTOR inhibition alleviates mitochondrial disease in a mouse model of Leigh syndrome. Science. 2013; 342 (6165):1524–8. Epub 2013/11/16. https://doi.org/10.1126/science.1244360 PMID: 24231806; PubMed Central PMCID: PMCPMC4055856.

8. Kayser EB, Sedensky MM, Morgan PG. Region-Specific Defects of Respiratory Capacities in the Ndufs4(KO) Mouse Brain. PLoS One. 2016; 11(1):e0148219. Epub 2016/01/30. https://doi.org/10.1371/journal.pone.0148219 PMID: 26824698; PubMed Central PMCID: PMCPMC4732614.

9. Zimin PI, Woods CB, Quintana A, Ramirez JM, Morgan PG, Sedensky MM. Glutamatergic Neurotransmission Links Sensitivity to Volatile Anesthetics with Mitochondrial Function. Curr Biol. 2016; 26 (16):2194–201. https://doi.org/10.1016/j.cub.2016.06.020 PMID: 27498564; PubMed Central PMCID: PMCPMC5007115.

10. Alkire MT, Haier RJ, Shah NK, Anderson CT. Positron emission tomography study of regional cerebral metabolism in humans during isoflurane anesthesia. Anesthesiology. 1997; 86(3):549–57. Epub 1997/03/01. PMID: 9066320.

11. Bonhomme V, Fiset P, Meuret P, Backman S, Plourde G, Paus T, et al. Propofol anesthesia and cerebral blood flow changes elicited by vibrotactile stimulation: a positron emission tomography study. J Neurophysiol. 2001; 85(3):1299–308. Epub 2001/03/15. PMID: 11247998.

12. Fiset P, Paus T, Daloze T, Plourde G, Meuret P, Bonhomme V, et al. Brain mechanisms of propofol-induced loss of consciousness in humans: a positron emission tomographic study. J Neurosci. 1999; 19 (13):5506–13. Epub 1999/06/23. PMID: 10377359.

13. Reinsel RA, Veselis RA, Dnistrian AM, Feshchenko VA, Beattie BJ, Duff MR. Midazolam decreases cerebral blood flow in the left prefrontal cortex in a dose-dependent fashion. Int J Neuropsychopharmacol. 2000; 3(2):117–27. Epub 2001/05/10. https://doi.org/10.1017/S1461145700001814 PMID: 11343588.

14. Veselis RA, Feshchenko VA, Reinsel RA, Dnistrian AM, Beattie B, Akhurst TJ. Thiopental and propofol affect different regions of the brain at similar pharmacologic effects. Anesth Analg. 2004; 99(2):399–408, table of contents. Epub 2004/07/24. https://doi.org/10.1213/01.ANE.0000131971.92180.DF PMID: 15271714.

15. Shulman RG, Hyder F, Rothman DL. Baseline brain energy supports the state of consciousness. Proc Natl Acad Sci U S A. 2009; 106(27):11096–101. Epub 2009/06/25. https://doi.org/10.1073/pnas.0903941106 PMID: 19549837; PubMed Central PMCID: PMCPMC2708743.

16. Laureys S, Lemaire C, Maquet P, Phillips C, Franck G. Cerebral metabolism during vegetative state and after recovery to consciousness. J Neurol Neurosurg Psychiatry. 1999; 67(1):121. Epub 1999/08/24. PMID: 10454871; PubMed Central PMCID: PMCPMC1736451.

17. Devor M, Zalkind V. Reversible analgesia, atonia, and loss of consciousness on bilateral intracerebral microinjection of pentobarbital. Pain. 2001; 94(1):101–12. Epub 2001/09/29. PMID: 11576749.

18. Antognini JF, Schwartz K. Exaggerated anesthetic requirements in the preferentially anesthetized brain. Anesthesiology. 1993; 79(6):1244–9. PMID: 8267200.

19. Akeju O, Loggia ML, Catana C, Pavone KJ, Vazquez R, Rhee J, et al. Disruption of thalamic functional connectivity is a neural correlate of dexmedetomidine-induced unconsciousness. Elife. 2014; 3:e04499. Epub 2014/11/29. https://doi.org/10.7554/eLife.04499 PMID: 25432022; PubMed Central PMCID: PMCPMC4280551.

20. Quintana A, Kruse SE, Kapur RP, Sanz E, Palmiter RD. Complex I deficiency due to loss of Ndufs4 in the brain results in progressive encephalopathy resembling Leigh syndrome. Proc Natl Acad Sci U S A. 2010; 107(24):10996–1001. Epub 2010/06/11. https://doi.org/10.1073/pnas.1006214107 PMID: 20534480; PubMed Central PMCID: PMC2890717.

21. Karunadharma PP, Basisty N, Chiao YA, Dai DF, Drake R, Levy N, et al. Respiratory chain protein turnover rates in mice are highly heterogeneous but strikingly conserved across tissues, ages, and treatments. Faseb j. 2015; 29(8):3582–92. Epub 2015/05/16. https://doi.org/10.1096/fj.15-272666 PMID: 25977255; PubMed Central PMCID: PMCPMC4511201.

22. Carriot J, Brooks JX, Cullen KE. Multimodal integration of self-motion cues in the vestibular system: active versus passive translations. J Neurosci. 2013; 33(50):19555–66. Epub 2013/12/18. https://doi.org/10.1523/JNEUROSCI.3051-13.2013 PMID: 24336720; PubMed Central PMCID: PMCPMC3858625.

23. Beitz AJ, Clements JR, Ecklund LJ, Mullett MM. The nuclei of origin of brainstem enkephalin and cholecystokinin projections to the spinal trigeminal nucleus of the rat. Neuroscience. 1987; 20(2):409–25. Epub 1987/02/01. PMID: 3295585.

24. Lein ES, Hawrylycz MJ, Ao N, Ayres M, Bensinger A, Bernard A, et al. Genome-wide atlas of gene expression in the adult mouse brain. Nature. 2007; 445(7124):168–76. Epub 2006/12/08. https://doi.org/10.1038/nature05453 PMID: 17151600.

25. Alkire MT, Haier RJ, Barker SJ, Shah NK, Wu JC, Kao YJ. Cerebral metabolism during propofol anesthesia in humans studied with positron emission tomography. Anesthesiology. 1995; 82(2):393–403; discussion 27A. Epub 1995/02/01. PMID: 7856898.

26. Baker R, Gent TC, Yang Q, Parker S, Vyssotski AL, Wisden W, et al. Altered activity in the central medial thalamus precedes changes in the neocortex during transitions into both sleep and propofol anesthesia. J Neurosci. 2014; 34(40):13326–35. Epub 2014/10/03. https://doi.org/10.1523/JNEUROSCI.1519-14.2014 PMID: 25274812; PubMed Central PMCID: PMCPMC4180471.

27. Wang N, Zhang Y, Wang JY, Gao G, Luo F. Effects of pentobarbital anesthesia on nociceptive processing in the medial and lateral pain pathways in rats. Neurosci Bull. 2010; 26(3):188–96. Epub 2010/05/27. https://doi.org/10.1007/s12264-010-0150-x PMID: 20502496; PubMed Central PMCID: PMCPMC4386992.

28. Oh SW, Harris JA, Ng L, Winslow B, Cain N, Mihalas S, et al. A mesoscale connectome of the mouse brain. Nature. 2014; 508(7495):207–14. Epub 2014/04/04. https://doi.org/10.1038/nature13186 PMID: 24695228; PubMed Central PMCID: PMCPMC5102064.

29. Kayser EB, Suthammarak W, Morgan PG, Sedensky MM. Isoflurane selectively inhibits distal mitochondrial complex I in Caenorhabditis elegans. Anesth Analg. 2011; 112(6):1321–9. Epub 2011/04/07. https://doi.org/10.1213/ANE.0b013e3182121d37 PMID: 21467554; PubMed Central PMCID: PMCPMC3102776.

30. Ries CR, Puil E. Mechanism of anesthesia revealed by shunting actions of isoflurane on thalamocortical neurons. J Neurophysiol. 1999; 81(4):1795–801. Epub 1999/04/14. PMID: 10200213.

31. Kayser EB, Morgan PG, Hoppel CL, Sedensky MM. Mitochondrial expression and function of GAS-1 in Caenorhabditis elegans. J Biol Chem. 2001; 276(23):20551–8. Epub 2001/03/30. https://doi.org/10.1074/jbc.M011066200 PMID: 11278828.

32. Pathak D, Shields L, Mendelsohn BA, Haddad D, Lin W, Gerencser AA, et al. The Role of Mitochondrially Derived ATP in Synaptic Vesicle Recycling. J Biol Chem. 2015. https://doi.org/10.1074/jbc.M115.656405 PMID: 26126824.

33. Sobieski C, Fitzpatrick MJ, Mennerick SJ. Differential Presynaptic ATP Supply for Basal and High-Demand Transmission. J Neurosci. 2017; 37(7):1888–99. https://doi.org/10.1523/JNEUROSCI.2712-16.2017 PMID: 28093477; PubMed Central PMCID: PMCPMC5320616.

34. Lenaz G, Fato R, Genova ML, Bergamini C, Bianchi C, Biondi A. Mitochondrial Complex I: structural and functional aspects. Biochim Biophys Acta. 2006; 1757(9–10):1406–20. Epub 2006/07/11. https://doi.org/10.1016/j.bbabio.2006.05.007 PMID: 16828051.

35. Lenaz G, D'Aurelio M, Merlo Pich M, Genova ML, Ventura B, Bovina C, et al. Mitochondrial bioenergetics in aging. Biochim Biophys Acta. 2000; 1459(2–3):397–404. Epub 2000/09/27. PMID: 11004456.

36. Herrera CG, Cadavieco MC, Jego S, Ponomarenko A, Korotkova T, Adamantidis A. Hypothalamic feed-forward inhibition of thalamocortical network controls arousal and consciousness. Nat Neurosci. 2016; 19(2):290–8. Epub 2015/12/23. https://doi.org/10.1038/nn.4209 PMID: 26691833.

37. Alkire MT, Haier RJ, Fallon JH. Toward a unified theory of narcosis: brain imaging evidence for a thalamocortical switch as the neurophysiologic basis of anesthetic-induced unconsciousness. Conscious Cogn. 2000; 9(3):370–86. Epub 2000/09/20. https://doi.org/10.1006/ccog.1999.0423 PMID: 10993665.

38. Jinks SL, Bravo M, Hayes SG. Volatile anesthetic effects on midbrain-elicited locomotion suggest that the locomotor network in the ventral spinal cord is the primary site for immobility. Anesthesiology. 2008; 108(6):1016–24. Epub 2008/05/24. https://doi.org/10.1097/ALN.0b013e3181730297 PMID: 18497602; PubMed Central PMCID: PMCPMC2713759.

39. Frank GB, Jhamandas K. Effects of drugs acting alone and in combination on the motor activity of intact mice. Br J Pharmacol. 1970; 39(4):696–706. Epub 1970/08/01. PMID: 4394969; PubMed Central PMCID: PMCPMC1702733.

40. MacIver MB, Bland BH. Chaos analysis of EEG during isoflurane-induced loss of righting in rats. Front Syst Neurosci. 2014; 8:203. Epub 2014/11/02. https://doi.org/10.3389/fnsys.2014.00203 PMID: 25360091; PubMed Central PMCID: PMCPMC4199270.

41. Alkire MT, Miller J. General anesthesia and the neural correlates of consciousness. Prog Brain Res. 2005; 150:229–44. Epub 2005/09/28. https://doi.org/10.1016/S0079-6123(05)50017-7 PMID: 16186027.

42. Shin TJ, Cho D, Ham J, Choi DH, Kim S, Jeong S, et al. Changes in thalamo-frontal interaction under different levels of anesthesia in rats. Neurosci Lett. 2016; 627:18–23. Epub 2016/05/28. https://doi.org/10.1016/j.neulet.2016.05.045 PMID: 27230989.

43. Lee CC, Sherman SM. Synaptic properties of thalamic and intracortical inputs to layer 4 of the first- and higher-order cortical areas in the auditory and somatosensory systems. J Neurophysiol. 2008; 100(1):317–26. Epub 2008/04/26. https://doi.org/10.1152/jn.90391.2008 PMID: 18436628; PubMed Central PMCID: PMCPMC2493493.

44. Sherman SM. Thalamus plays a central role in ongoing cortical functioning. Nat Neurosci. 2016; 16 (4):533–41. Epub 2016/03/30. https://doi.org/10.1038/nn.4269 PMID: 27021938.

45. Feng D, Lau C, Ng L, Li Y, Kuan L, Sunkin SM, et al. Exploration and visualization of connectivity in the adult mouse brain. Methods. 2015; 73:90–7. Epub 2015/02/01. https://doi.org/10.1016/j.ymeth.2015.01.009 PMID: 25637033.

46. Cunningham SI, Tomasi D, Volkow ND. Structural and functional connectivity of the precuneus and thalamus to the default mode network. Hum Brain Mapp. 2017; 38(2):938–56. Epub 2016/10/16. https://doi.org/10.1002/hbm.23429 PMID: 27739612.

47. Vanhaudenhuyse A, Noirhomme Q, Tshibanda LJ, Bruno MA, Boveroux P, Schnakers C, et al. Default network connectivity reflects the level of consciousness in non-communicative brain-damaged patients. Brain. 2010; 133(Pt 1):161–71. Epub 2009/12/26. https://doi.org/10.1093/brain/awp313 PMID: 20034928; PubMed Central PMCID: PMCPMC2801329.

48. Boly M, Phillips C, Tshibanda L, Vanhaudenhuyse A, Schabus M, Dang-Vu TT, et al. Intrinsic brain activity in altered states of consciousness: how conscious is the default mode of brain function? Ann N Y Acad Sci. 2008; 1129:119–29. Epub 2008/07/02. https://doi.org/10.1196/annals.1417.015 PMID: 18591474; PubMed Central PMCID: PMCPMC2855379.

49. Merighi A, Salio C, Ghirri A, Lossi L, Ferrini F, Betelli C, et al. BDNF as a pain modulator. Prog Neurobiol. 2008; 85(3):297–317. Epub 2008/06/03. https://doi.org/10.1016/j.pneurobio.2008.04.004 PMID: 18514997.

50. Frias B, Merighi A. Capsaicin, Nociception and Pain. Molecules. 2016; 21(6). Epub 2016/06/21. https://doi.org/10.3390/molecules21060797 PMID: 27322240.

51. Delevich K, Tucciarone J, Huang ZJ, Li B. The mediodorsal thalamus drives feedforward inhibition in the anterior cingulate cortex via parvalbumin interneurons. J Neurosci. 2015; 35(14):5743–53. Epub 2015/04/10. https://doi.org/10.1523/JNEUROSCI.4565-14.2015 PMID: 25855185; PubMed Central PMCID: PMCPMC4388929.

52. Sherrington CS. The integrative action of the nervous system. New Haven, CT: Yale University Press; 1906.

53. Porreca F, Ossipov MH, Gebhart GF. Chronic pain and medullary descending facilitation. Trends Neurosci. 2002; 25(6):319–25. Epub 2002/06/28. PMID: 12086751.

54. Ren K, Dubner R. Descending modulation in persistent pain: an update. Pain. 2002; 100(1–2):1–6. Epub 2002/11/19. PMID: 12435453.

55. King BS, Rampil IJ. Anesthetic depression of spinal motor neurons may contribute to lack of movement in response to noxious stimuli. Anesthesiology. 1994; 81(6):1484–92. Epub 1994/12/01. PMID: 7992918.

56. Rampil IJ, King BS. Volatile anesthetics depress spinal motor neurons. Anesthesiology. 1996; 85 (1):129–34. Epub 1996/07/01. PMID: 8694358.

57. Spangler-Bickell MG, de Laat B, Fulton R, Bormans G, Nuyts J. The effect of isoflurane on 18F-FDG uptake in the rat brain: a fully conscious dynamic PET study using motion compensation. EJNMMI Res. 2016; 6(1):86. Epub 2016/11/27. https://doi.org/10.1186/s13550-016-0242-3 PMID: 27888500; PubMed Central PMCID: PMCPMC5124015.

58. Gupta RG, Schafer C, Ramaroson Y, Sciullo MG, Horn CC. Role of the abdominal vagus and hindbrain in inhalational anesthesia-induced vomiting. Auton Neurosci. 2017; 202:114–21. Epub 2016/07/12. https://doi.org/10.1016/j.autneu.2016.06.007 PMID: 27396693; PubMed Central PMCID: PMCPMC5203944.

59. Fadok JP, Dickerson TM, Palmiter RD. Dopamine is necessary for cue-dependent fear conditioning. J Neurosci. 2009; 29(36):11089–97. Epub 2009/09/11. https://doi.org/10.1523/JNEUROSCI.1616-09.2009 PMID: 19741115; PubMed Central PMCID: PMCPMC2759996.

60. Bruchas MR, Schindler AG, Shankar H, Messinger DI, Miyatake M, Land BB, et al. Selective p38alpha MAPK deletion in serotonergic neurons produces stress resilience in models of depression and addiction. Neuron. 2011; 71(3):498–511. Epub 2011/08/13. https://doi.org/10.1016/j.neuron.2011.06.011 PMID: 21835346; PubMed Central PMCID: PMCPMC3155685.

61. Zweifel LS, Argilli E, Bonci A, Palmiter RD. Role of NMDA receptors in dopamine neurons for plasticity and addictive behaviors. Neuron. 2008; 59(3):486–96. Epub 2008/08/15. https://doi.org/10.1016/j.neuron.2008.05.028 PMID: 18701073; PubMed Central PMCID: PMCPMC2556153.

62. Sonner JM, Werner DF, Elsen FP, Xing Y, Liao M, Harris RA, et al. Effect of isoflurane and other potent inhaled anesthetics on minimum alveolar concentration, learning, and the righting reflex in mice engineered to express alpha1 gamma-aminobutyric acid type A receptors unresponsive to isoflurane. Anesthesiology. 2007; 106(1):107–13. PMID: 17197852.

63. Morgan SE, Frink EJ, Gandolfi AJ. A simplified gas chromatographic method for quantifying the sevoflurane metabolite hexafluoroisopropanol. Anesthesiology. 1994; 80(1):201–5. Epub 1994/01/01. PMID: 8291710.

64. Song L, Cortopassi G. Mitochondrial complex I defects increase ubiquitin in substantia nigra. Brain Res. 2015; 1594:82–91. Epub 2014/12/03. https://doi.org/10.1016/j.brainres.2014.11.013 PMID: 25446449.